Infection of the Biomphalaria glabrata vector snail by Schistosoma mansoni parasites drives snail microbiota dysbiosis

Anaïs Portet, Eve Toulza, Ana Lokmer, Camille Huot, David Duval, Richard Galinier, Benjamin Gourbal

▶ **To cite this version:**

Anaïs Portet, Eve Toulza, Ana Lokmer, Camille Huot, David Duval, et al.. Infection of the Biomphalaria glabrata vector snail by Schistosoma mansoni parasites drives snail microbiota dysbiosis. 2018. hal-03134818

HAL Id: hal-03134818
https://hal.science/hal-03134818

Preprint submitted on 11 Feb 2021

HAL is a multi-disciplinary open access archive for the deposit and dissemination of scientific research documents, whether they are published or not. The documents may come from teaching and research institutions in France or abroad, or from public or private research centers.

L'archive ouverte pluridisciplinaire **HAL**, est destinée au dépôt et à la diffusion de documents scientifiques de niveau recherche, publiés ou non, émanant des établissements d'enseignement et de recherche français ou étrangers, des laboratoires publics ou privés.

bioRxiv preprint doi: https://doi.org/10.1101/386623; this version posted June 4, 2019. The copyright holder for this preprint (which was not certified by peer review) is the author/funder. All rights reserved. No reuse allowed without permission.

Infection of the *Biomphalaria glabrata vector snail* by *Schistosoma mansoni* parasites drives snail microbiota dysbiosis.

Anaïs Portet [1], Eve Toulza [1], Ana Lokmer [2], Camille Huot [1], David Duval [1], Richard Galinier [1] and Benjamin Gourbal [1, §]

[1] IHPE, Univ. Montpellier, CNRS, Ifremer, Univ. Perpignan Via Domitia, Perpignan France

[2] Department Coastal Ecology, Wadden Sea Station Sylt, Alfred Wegener Institute, Helmholtz Centre for Polar and Marine Research, List/Sylt, Germany.

AP: ap2133@cam.ac.uk, ET: eve.toulza@univ-perp.fr, AL: Ana.Lokmer@awi.de, CH: camillehuot86@gmail.com, DD: david.duval@univ-perp.fr, RG: richard.galinier@univ-perp.fr, BG: benjamin.gourbal@univ-perp.fr

[§] Corresponding author :

Benjamin GOURBAL

UMR5244 IHPE, Université de Perpignan

58 avenue Paul Alduy, 66860 Perpignan

benjamin.gourbal@univ-perp.fr

Running title: Biomphalaria glabrata snail microbiota dysbiosis

bioRxiv preprint doi: https://doi.org/10.1101/386623; this version posted June 4, 2019. The copyright holder for this preprint (which was not certified by peer review) is the author/funder. All rights reserved. No reuse allowed without permission.

Summary

Host-associated microbiota can affect the fitness of its host in a number of ways, including the modification of host-parasite interactions and thus the outcome of disease. *Biomphalaria glabrata* is the vector snail of the trematode *Schistosoma mansoni*, the agent of human schistosomiasis, causing hundreds of thousands of deaths every year. Here, we present the first study of the snail bacterial microbiota in response to *Schistosoma* infection. To examine the interplay between *B. glabrata, S. mansoni* and snail microbiota, snails were infected and the microbiota composition was analysed by massive 16S rDNA amplicon sequencing approach. We characterized the *Biomphalaria* bacterial microbiota at the individual level in both naïve and infected snails. Sympatric and allopatric strains of parasites were used for infections and re-infections to analyse the modification or dysbiosis of snail microbiota in different host-parasite co-evolutionary contexts. Concomitantly, using RNAseq data, we investigated the link between bacterial microbiota dysbiosis and snail anti-microbial peptide immune response. This work paves the way for a better understanding of snail/schistosome interaction, and would have critical consequences in terms of snail control strategies for fighting schistosomiasis disease in the field.

Key words: microbiota; bacteria; *Biomphalaria* snail; *Schistosoma* infection; immune response; dysbiosis

bioRxiv preprint doi: https://doi.org/10.1101/386623; this version posted June 4, 2019. The copyright holder for this preprint (which was not certified by peer review) is the author/funder. All rights reserved. No reuse allowed without permission.

Introduction

Several studies have shown that the microbiota interacts with pathogens and/or host immunity in invertebrates. For example, the midgut microbiota of the mosquito *Aedes sp.* elicits a basal immune activity of the immune system (Ramirez et al., 2012) mostly by activating Toll pathways (Xi et al., 2008). In *Anopheles gambiae*, some members of its microbiota can limit malaria transmission, by inducing a wide antimicrobial immune response (Gendrin, 2017). More precisely, bacteria of the genus *Enterobacter*, found in the mosquito microbiota, were shown to produce reactive oxygen species (ROS) that inhibit *Plasmodium* development (Cirimotich et al., 2011). Furthermore, the endosymbiotic bacteria *Wolbachia* induce expression of immune genes, like TEP1 (Thioester-containing protein 1), LRIM1 (Leucine-Rich Immune Molecule 1) or defensin 1 (Joshi et al., 2017). In *Drosophila*, the bacterial microbiota is necessary to produce the Pvf2, a PDGF/VEGF-like growth factor that restricts enteric viral infection (Sansone et al., 2015). The microbiota may also play a role in immune priming. For example, in *Anopheles gambiae*, hemocyte priming during the *Plasmodium* infection is naturally induced by the gut microbiota, whose absence results in more severe infections and re-infections (Rodrigues et al., 2010). Similarly, the gut microbiota is necessary for immune priming in *Tribolium castaneum* and efficient response against *Bacillus thuringiensis for Tenebrionis* (Futo et al., 2015). Finally, host immunity can influence the tolerance or control the microbiota. In the tick *Ixodes scapularis*, the protein PIXR, secreted by the tick's gut, inhibits the bacterial biofilm formation and supports gut eubiosis (healthy gut microbiota), its inactivation leading to dysbiosis. This change in gut microbiota facilitates the colonization by *Borrelia burgdorferi*, the Lyme disease agent (Narasimhan et al., 2017). In *Drosophila,* for example, the intestinal homeobox gene Caudal regulates the commensal-gut mutualism by repressing nuclear factor kappa B-

bioRxiv preprint doi: https://doi.org/10.1101/386623; this version posted June 4, 2019. The copyright holder for this preprint (which was not certified by peer review) is the author/funder. All rights reserved. No reuse allowed without permission.

dependent antimicrobial peptide genes (Ryu et al., 2008). In Hydra, the innate immune sensors and effectors protect not only against pathogens but also control microbiota homeostasis (Augustin et al., 2010). Moreover, host specific antimicrobial peptides (Fraune et al., 2010; Franzenburg et al., 2012) and a rich repertoire of pattern recognition receptors (Bosch, 2013) are involved in maintaining homeostasis between the host and the resident microbiota. Similarly, bactericidal permeability-increasing proteins (BPIs) shape bacterial communities in the light organ of the squid *Euprymna scolopes* and prevent their spill over to other tissues (Chen et al., 2017).

Biomphalaria glabrata is a freshwater snail (Lophotrochozoa, Planorbidae), living in inter-tropical regions of Latin America, in rivers, ponds, waterways and other freshwater environments. *B. glabrata* snails have important medical and epidemiological impacts due to their role as the main vector of *Schistosoma mansoni* (Lophotrochozoa, Platyhelminthes, Trematoda), the agent of intestinal schistosomiasis. Schistosomiasis is the second most widespread human parasitic disease after malaria, affecting over 200 million people worldwide and causing 200 000 deaths annually (WHO, 2002). The *Schistosoma* adult parasites mate in the human host venous system. Female worms produce eggs that cross endothelial mesenteric vessels and intestinal epithelium to reach faeces and finally the aquatic environment. Once in the water, eggs hatch and release miracidia, the free-living snail-infective parasite stage. At the following step of the life cycle, the miracidium needs to infect the freshwater snail *B. glabrata*. Intensive asexual multiplication in the snail tissues leads to the continuous production of hundreds of generations of cercariae, the free-living human-infective parasite stage.

At present, there is no effective vaccine against schistosomiasis and the treatment relies on a single chemotherapeutic treatment, the Praziquantel (Doenhoff et al., 2009), against which

bioRxiv preprint doi: https://doi.org/10.1101/386623; this version posted June 4, 2019. The copyright holder for this preprint (which was not certified by peer review) is the author/funder. All rights reserved. No reuse allowed without permission.

resistance has been observed (Fallon and Doenhoff, 1994). Molluscicides have been also used to impair *Schistosoma* transmission in the field. However, the dramatic effects of molluscicides on natural environments prompt us to seek new ways to prevent and / or control this disease in the field (Tennessen et al., 2015). We propose that a better understanding of ecological interactions between, *Schistosoma mansoni, Biomphalaria glabrata* snails and its associated microbiota might represent an interesting approach in search for alternative control strategies.

In this context, we have conducted numerous studies on immunological interactions between the snail and the parasite (Mitta et al., 2005; Bouchut et al., 2008; Moné et al., 2011; Coustau et al., 2015; Galinier et al., 2017; Mitta et al., 2017). We have demonstrated that the nature of the snail immune response depends on the strain/species of host or of parasite considered. Depending on both the host and the parasite intrinsic capacities, parasites either develop normally in snail tissue (compatible interaction) or are encapsulated by hemocytes (the snail immune cells) (incompatible interaction) (Mone et al., 2010; Mitta et al., 2012; Coustau et al., 2015) (Fig. 1). Depending on the ecological context, totally different immunobiological interactions have been described in *B. glabrata/S. mansoni* interactions. If immunosuppression occurs during a sympatric interaction, an activation of the immune response is observed during an allopatric interaction (Portet et al., 2019). Moreover, following primo-infection and successive challenges, a shift from a cellular immune response toward a humoral immune response has been described (Pinaud et al., 2016) (Fig. 1).

However, in the present host-parasite model, only few studies examined the bacterial microbiota of *Biomphalaria glabrata* so far (Ducklow et al., 1979; Silva et al., 2013). The study of aerobic heterotrophic cultivable flora of 200 snails (Ducklow et al., 1979) revealed five predominant bacterial genera including *Pseudomonas, Acinetobacter, Aeromonas, Vibrio* and

bioRxiv preprint doi: https://doi.org/10.1101/386623; this version posted June 4, 2019. The copyright holder for this preprint (which was not certified by peer review) is the author/funder. All rights reserved. No reuse allowed without permission.

114 *Enterobacter*. In a more recent study, the *Biomphalaria glabrata* bacterial microbiota has been
115 characterized using 16S rRNA sequences (Silva et al., 2013) of cultured isolates, identifying six
116 additional bacteria genera: *Citrobacter, Cupriavidus, Rhizobium, Stenotrophomonas, Klebsiella*
117 and *Sphingomonas*. In addition, diversity and composition of bacterial microbiota differed
118 between resistant and susceptible *Biomphalaria* phenotypes, with differences in relative
119 abundances of *Gemmatimonas aurantiaca* and *Micavibrio aeruginosavorus*. This observation
120 supports the potential link between the resistance against *Schistosoma* parasite and the
121 structure of snail-associated microbiota (Allan et al., 2018). However, no studies have examined
122 changes in bacterial microbiota of *Biomphalaria* snails by culture-independent methods nor
123 following Schistosoma infections so far.
124 Taking into account all the peculiarities of this system, the aim of the present study was to
125 investigate variation of microbiota in snail populations as well as to assess the influence of
126 varying immune response against *Schistosoma* on the host microbiota composition and
127 dynamics. To reach this goal, we first characterized the bacterial microbiota of naive
128 *Biomphalaria glabrata* snails using 16S rDNA metabarcoding. Then, we analysed changes in
129 microbiota composition following, (i) primo-infections with sympatric and allopatric *S. mansoni*
130 parasite isolates displaying the same prevalence and intensity phenotypes and, (ii) subsequent
131 secondary challenges with homologous or heterologous parasite strains. As snail immune
132 response strongly differs between such diverse snail/parasite combinations, we concomitantly
133 analysed the snail immune response using a massive sequencing transcriptomic approach
134 (RNAseq) in order to link it with the observed changes in the composition and diversity of the
135 microbiota.
136

bioRxiv preprint doi: https://doi.org/10.1101/386623; this version posted June 4, 2019. The copyright holder for this preprint (which was not certified by peer review) is the author/funder. All rights reserved. No reuse allowed without permission.

Results

Characterization of healthy B. glabrata *microbiota*

To examine the stability of naive BgBRE snail microbiota, we first inspected the microbiota diversity and composition in the control naive snails at day 0 and 25 of the experiment. We found no significant differences between the B0 and B25 snails in any of the alpha diversity indices (Table S3, Table S4).

Naive snails showed little inter-individual variability and a stable composition at the phylum level over time (Fig. 2A, Table S3, Table S4), with Proteobacteria, Bacteroidetes, Cyanobacteria and Planctomycetes phyla being the most represented (Fig 2A). Moreover, the bacterial microbiota of naïve BgBRE snails displayed a considerable temporal and inter-individual stability at the family level (Fig. 2B). The stability of naïve snail microbiota composition over time (Fig. 2) could be related to the laboratory rearing conditions and laboratory environmental abiotic variables (water composition, temperature, pH, food) that were tidily controlled and that did thus not result in changes in host snail physiology or metabolism.

In terms of composition, we observed that 67 (69%) and 86 (89%) out of 97 identified families were shared by all individuals of B0 or B25 naive snails respectively (Fig. 2B). Those results were used to determine the core microbiota. We defined core microbiota as the families that were present in 100% of the naive snails. Applying this definition, we identified 62 out of 97 families found in all naive individual snails (B0 and B25 altogether), and thus constituting the *B. glabrata* core-microbiota (Table S7 and S8).

Microbiota dynamics following B. glabrata *infections by* S. mansoni

bioRxiv preprint doi: https://doi.org/10.1101/386623; this version posted June 4, 2019. The copyright holder for this preprint (which was not certified by peer review) is the author/funder. All rights reserved. No reuse allowed without permission.

160 After establishing the stability of naive *Biomphalaria* bacterial microbiota, we investigated
161 whether *Schistosoma mansoni* infections affected the microbiota structure and dynamics.
162 To investigate the influence of parasite infections on the bacterial microbiota, we analysed
163 microbiota dynamics following sympatric or allopatric primo-infections and homologous or
164 heterologous challenges (Fig. 1).
165
166 We did not observe any significant changes in alpha diversity during the course of primo-
167 infection compared to naive snails, excepted a decrease in the Shannon's H diversity index at
168 the fourth day after sympatric infection (Fig. 3, Table S3, Mann-Whitney U test: Table S4).
169 Conversely, all indices changed significantly following homologous or heterologous challenges
170 (Fig. 3, Table S3, Table S4). Indeed, the observed species richness (Mann-Whitney U test,
171 p=0.002), the Chao 1 richness index (Mann-Whitney U test, p=0.006), Shannon diversity index
172 (p=0.0004) and Pielou evenness index (Mann-Whitney U test, p=0.009) were significantly
173 reduced following homologous or heterologous challenges compared to naive and primo-
174 infected snails (Fig. 3, Table S3, Table S4). However, the observed drop in alpha diversity
175 disappeared by the fourth day after heterologous challenge (Fig. 3, Table S4). In addition, alpha
176 diversity was mainly affected by the challenge, regardless of its type (homologous or
177 heterologous). The primo-infection did not significantly affect alpha diversity except for the
178 sympatric combination at day 4 after infection (Table S4).
179 Regarding the beta diversity, Principal Coordinate Analysis (PCoA) of Bray-Curtis dissimilarities
180 revealed that BB25 samples grouped together with the naive snail samples (B0 and B25) and
181 were separated from the infected-snail samples along both axes (Fig. 4A, Table S5). However,
182 the BB25 samples were significantly different from the naive snail samples (Table S5). The fact

bioRxiv preprint doi: https://doi.org/10.1101/386623; this version posted June 4, 2019. The copyright holder for this preprint (which was not certified by peer review) is the author/funder. All rights reserved. No reuse allowed without permission.

183 that, BB25 grouped with naive snails rather than with infected-snail samples suggests that the
184 snail microbiota is resilient to infection, with a tendency to recover between day 4 and day 25
185 after the primo-infection (Fig. 4A). Analysis of Bray-Curtis dissimilarity index revealed a
186 significant difference between naive and primo-infected samples (p=0.001) and also between
187 naive and challenged samples (p=0.001) (Table S5). Concerning the infected-snail samples, all
188 experimental samples were significantly different from each other with the exception of BB1
189 versus BB4 and BBB1 versus BBV1 (Table S5).
190 In addition, the second PcoA axis separated the samples according to the course of infection
191 (i.e. the day 1 from the day 4 samples) (Fig. 4A), whereas the day 1 after-challenge (BBB1,
192 BBV1), the day 1 after-primo-infection (BB1, BV1) and all of the day 4 infection samples (BB4,
193 BV4, BBB4, BBV4) were separated along the first axis (Fig. 4A). Interestingly, day 1 after-
194 challenge samples (BBB1, BBV1) were more different from the naive microbial communities
195 than the day 1 primo-infection samples (BB1, BV1). Moreover, the second axis separated the
196 sympatric primo-infection (BB1) from the allopatric primo-infection (BV1) (Fig. 4A). Finally, all
197 day 4 samples grouped together reflecting the similarity between these samples regardless of
198 experimental infection conditions (Fig. 4A). Even if the day of infection appears as the main
199 explaining factor, these results indicate that the snail microbiota response to the infection also
200 depends on the type of infection (sympatric vs. allopatric or primo-infection vs. challenge) and
201 suggest the existence of predictable dynamics.
202
203 We further investigated the microbial community dynamics following infection, and we
204 observed some consistent changes in response to experimental infection type (Fig. 4B). The
205 relative abundance of Tenericutes increased after infection, particularly at day 1 after challenge

bioRxiv preprint doi: https://doi.org/10.1101/386623; this version posted June 4, 2019. The copyright holder for this preprint (which was not certified by peer review) is the author/funder. All rights reserved. No reuse allowed without permission.

206 (BB25 vs BBB1, student T test P = 0.0114; BB25 vs BBV1 student T test P = 0.0209). Increase in
207 Verrucomicrobia following allopatric primo-infection (B0/B25 vs BV4, student T test P = 6.53 e-
208 06) and homologous / heterologous challenge (B0/B25 vs BBB4/BBV4, student T test P =
209 0.0012) was most prominent at day 4 after infection (Fig. 4B). Interestingly, high relative
210 abundance of Verrucomicrobia in BB25 represents the main difference with naive snail
211 microbial community composition (B0/B25 vs BB25, student T test P = 1.83 e -05) (Fig. 4B). We
212 further observed decrease in Planctomycetes following sympatric primo-infection (B0/B25 vs
213 BB1/BB4, student T test P = 5.7 e-07) and a decrease in Cyanobacteria following allopatric
214 primo-infection (B0/B25 vs BV1/BV4, student T test P = 0.00254). Interestingly, the relative
215 abundance of both phyla decreased following the challenge regardless of the challenge type
216 (Planctomycetes B0/B25/BB25 vs BBB1/BBB4/BBV1/BBV4, student T test P = 0.0017 and
217 Cyanobacteria B0/B25/BB25 vs BBB1/BBB4/BBV1/BBV4, student T test P = 0.000568) (Fig. 4B).
218 Bacteroidetes decreased 25 days after sympatric primo-infection (B0/B25 vs BB25, student T
219 test P = 0.0467) but increased 4 days after heterologous challenge (BB25 vs BBV4, student T
220 test P = 0.00577). To conclude, depending on the phylum, we observed the largest
221 modifications in microbiota composition at day 1 or 4 after primo-infections and challenges.
222 Whereas the microbiota responded differently to sympatric and allopatric primo-infections, we
223 found no significant differences between the homologous or heterologous challenge (see BBB1
224 vs BBV1, Fig. 4) (Table S5).
225
226 Finally, we examined the core microbiota dynamics during infection. Similarly, to the complete
227 microbiota, the core-microbiota, consisting of 62 families, was affected by the type of infection
228 (naive vs primo-infection (p=0.003) and naive *vs* challenge (p=0.003)), by the time of infection

bioRxiv preprint doi: https://doi.org/10.1101/386623; this version posted June 4, 2019. The copyright holder for this preprint (which was not certified by peer review) is the author/funder. All rights reserved. No reuse allowed without permission.

(early (1 day) vs late (4 days)) (p=0.006) and also by the strain of parasite used for primo-infection (SmBRE vs SmVEN) (p=0.016) (Table S6). Principal Coordinate Analysis (PCoA) based on Bray-Curtis dissimilarities between the core microbiotas (Fig. S1) yielded very similar results to those based on the entire dataset (Fig. 4A).

In addition, we observed that 69.4% (43) of the core microbiota families were significantly affected by infection. Among those, 6.5% (4 families) were affected regardless of the infection type (Table S7). Interestingly, these families belong to the most abundant ones (Table S8). Nineteen families (30.6%) were never affected by infection (Table S7). Those families belong to the less represented ones, with the exception of *Xanthomonadaceae,* which was the 7th most represented family (see Table S8). Further 32.6% (14 families) of the core microbiota responded solely to the primo-infection and 4.7% (2 families) to the challenge (Table S7). Similarly, 20.9% (9 families) of the core microbiota was affected early after infection (1 day) and 7% later (3 families, day 4). Finally, 23.3% (10 families) were affected by the SmBRE infection and 9.3% (4 families) by the SmVEN infection (Table S7).

Link between the microbiota dysbiosis and B. glabrata *antimicrobial immune response*

The expression level of transcripts encoding antimicrobial peptides and antimicrobial proteins (AMP) was investigated following sympatric or allopatric primo-infection and homologous or heterologous challenges using RNAseq data (Fig. 5 and Fig. S2). Two achacin genes, 5 lipopolysaccharide-binding protein / bactericidal permeability-increasing protein (LBP/PBI) genes, and 5 biomphamacin genes were selected based on the *Biomphalaria glabrata* genome annotation (Adema et al., 2017). In comparison with the naive snails, the LBP/BPI 3.1 and 3.2 were over-expressed at day 25 after infection and following the challenges, while all other

bioRxiv preprint doi: https://doi.org/10.1101/386623; this version posted June 4, 2019. The copyright holder for this preprint (which was not certified by peer review) is the author/funder. All rights reserved. No reuse allowed without permission.

252 genes of this family were under-expressed in all conditions (Fig. S2). The achacins were under-
253 expressed following primo-infection in the sympatric combination only, and at day 25 after
254 primo-infection and following both challenges (Fig. S2). No changes in expression were
255 observed following allopatric primo-infection compared to the naive snails (Fig. S2). Finally, the
256 AMP biomphamacins 1, 4, 5 and 6 were over-expressed throughout the infection stages, except
257 for BV1 and BB25 (Fig.6). The biomphamacin 3 was mainly under-expressed except at BV4 and
258 BBB, where no differential expressions have been detected compared with naive snails (Fig. 5).
259
260 Based on our observations of microbial community shifts, changes in expression of
261 antimicrobial molecules were expected to occur following primo-infections and challenges and
262 not for BB25, where resilience of microbial communities has been observed (Fig. 4 and Fig. S1).
263 In this context, the LBP/BPI and achacin seem not to be linked with dysbiosis, as both remained
264 highly down regulated even at BB25 when communities had already recovered (Fig. S2). All
265 biomphamacins, except the biomphamacin 3, were over-expressed after infection, from day 1
266 in BB infection and day 4 in BV infection and for homologous or heterologous challenges (BBB
267 and BBV). Finally, only a subset of biomphamacins (1, 4, 5, 6) changed in the course of infection
268 but were not differentially expressed at BB25 compared with the naive snails (Fig. 5),
269 suggesting their possible link with dysbiosis.
270
271 **Discussion**
272 Fine-tuned interactions between microbiota, host immunity and pathogens have been
273 observed in many vertebrate and invertebrate models (Rodrigues et al., 2010; Ramirez et al.,
274 2012; Futo et al., 2015; Sansone et al., 2015; Chen et al., 2017). Following an infection by a

bioRxiv preprint doi: https://doi.org/10.1101/386623; this version posted June 4, 2019. The copyright holder for this preprint (which was not certified by peer review) is the author/funder. All rights reserved. No reuse allowed without permission.

pathogen, a host displays an innate or adaptive immune response against the intruder. The activation of such immune response may in turn affect the microbial community structure.

Herein, we investigated the interactions between the host immune system, parasite and the bacterial microbiota in an invertebrate model - the gastropod snail *Biomphalaria glabrata and its* trematode parasite *Schistosoma mansoni*. Depending on the past evolutionary history between snails and schistosomes, different immune responses against *S. mansoni* have been observed. We showed recently that in a sympatric interaction, the parasite that coevolved with its host induced a strong immunosuppression, whereas allopatric interaction resulted in a strong host cellular immune response (Portet et al., 2019). Moreover, a cellular immune response was observed following primo-infection, but a humoral immune response was observed following homologous or heterologous challenges (Pinaud et al., 2016). So using appropriate parasite-host combinations, we have the opportunity to modulate the host immune response type and to test changes in bacterial community composition and diversity (dysbiosis). First, studying the global bacterial microbiota community of *Biomphalaria* snails, we showed that the bacterial alpha diversity was not modified following primo-infection whatever the parasite strain or the time point of infection (Fig. 3, S3 Table). A decrease in alpha diversity is observed exclusively following challenge infections, as reflected by multiple indices (Fig. 3, S3 Table). Conversely, primo-infection and challenge strongly affected the bacterial OTU composition (Fig. 4). Moreover, differences in immunobiological interactions (immunosuppression, immune cellular response or immune humoral response) resulted in different microbiota dysbiosis reflected by specific changes in the snail microbial community (Fig. 4). Interestingly, homologous and heterologous challenges activated similar humoral immune response (Pinaud et al., 2016; Portet et al., 2019) that resulted in a similar change of

bioRxiv preprint doi: https://doi.org/10.1101/386623; this version posted June 4, 2019. The copyright holder for this preprint (which was not certified by peer review) is the author/funder. All rights reserved. No reuse allowed without permission.

298 microbiota alpha diversity and composition (Fig. 3, S3 Table, Fig. 4). Then, four days after
299 infection, regardless of its type, the microbiota was still very different from the one in the naïve
300 snails, but the differences between the primo-infection and challenge disappeared, as apparent
301 from the grouping of BB4, BV4, BBB4 and BBV4 in the PCoA (see Fig. 4). Furthermore, most of
302 the OTUs affected by the primo-infection, returned to their initial state by the day 25, indicating
303 that the snail microbiota is resilient against the infection (Fig. 4). However, some differences
304 persisted: the Verrucomicrobia phylum remained highly represented in the infected snails at
305 day 25 after primo-infection (Fig. 4B). Interestingly, some Verrucomicrobia species have been
306 recently proposed as a hallmark of healthy gut due to its anti-inflammatory and immune-
307 stimulant properties and its ability to improve gut barrier function (Fujio-Vejar et al., 2017).
308 High abundance of Verrucomicrobia in the recovered snails could thus potentially reflect their
309 role in community restoration (Fig. 4). Moreover, the expansion of a Verrucomicrobia species
310 *Akkermansia muciniphila*has been demonstrated in the gut of *S. mansoni*-infected mice,
311 suggesting a potentially functional role of Verrucomicrobia in *Schistosoma* infection processes
312 in both final and intermediate hosts (Jenkins et al., 2018). We also paid a particular attention to
313 the core-microbiota. Given the various ways to define core microbiota, we considered
314 exclusively the persistent occurrence in the bacterial community in naive *Biomphalaria glabrata*
315 snails (Astudillo-García et al., 2017). Similarly, to the entire microbiota, the core microbiota was
316 affected by the type of infection (naive *vs* challenge), by the time of infection (day 1 vs day 4) as
317 well as by the parasite strain (SmBRE vs SmVEN) (Table S6). Core microbiota seemed to be
318 affected by immunosuppression or the activation of the immune response in a similar way than
319 the whole microbiota (Fig. S1 and Fig. 4A). Understanding the shifts in core microbiota
320 following infection is important as the long-term stability and persistent occurrence of

bioRxiv preprint doi: https://doi.org/10.1101/386623; this version posted June 4, 2019. The copyright holder for this preprint (which was not certified by peer review) is the author/funder. All rights reserved. No reuse allowed without permission.

321 beneficial microbes and their associated functions may contribute to host health and well-being
322 to maintain host functionality and fitness toward changing ecological environment or
323 environmental stress (Nyholm and McFall-Ngai, 2004; Lozupone et al., 2012; McFall-Ngai et al.,
324 2013).

325 Given that infections affect the total and core microbiota structure, we explored the
326 antimicrobial immune response following infection to find potential molecular mechanisms
327 involved in the observed microbiota dysbiosis (Fig. 5 and Fig. S2). We analysed antimicrobial
328 peptides (AMP) and antimicrobial proteins and our results suggest that only the AMP belonging
329 to biomphamacin family may potentially affect the microbial communities in response to
330 *Schistosoma* infection. Indeed, even though antimicrobial families can be involved in complex
331 process of regulation or of control of microbiota communities, solely the biomphamacins AMP
332 family members specifically displayed an expression pattern that can be linked with the
333 observed dysbiosis of *Biomphalaria* bacterial communities (Fig. 5). Even if AMPs is often
334 considered as the main immune pathway responsible for microbiota regulation (Onchuru and
335 Kaltenpoth, 2019), an overall modification of the immune system may also be considered as a
336 cause of dysbiosis. The potential role of immune recognition or ROS/NOS pathways as to be
337 considered (Wang et al., 2014; Budachetri and Karim, 2015; Yang et al., 2015; Yang et al., 2016)
338 and this will deserve further investigations in the present biological experimental model.
339 It has been shown that the immune system is a key determinant of host-associated bacterial
340 communities in many biological systems. Two mechanisms have been proposed to explain host-
341 microbiota interactions through crosstalk with the host innate immune system. The first one
342 proposes that the host immune system exerts constant pressure on the microbiota in order to
343 maintain homeostasis (Hooper et al., 2012), the host immune system can thus control the

bioRxiv preprint doi: https://doi.org/10.1101/386623; this version posted June 4, 2019. The copyright holder for this preprint (which was not certified by peer review) is the author/funder. All rights reserved. No reuse allowed without permission.

344 composition of the resident microbiota (Zhang et al., 2015). According to this hypothesis, any
345 changes in host immune response to infection would potentially affect the resident microbiota
346 diversity and composition. The second mechanism proposes that the immune system would be
347 tolerant to weak and continuous antigenic immune stimulations experienced during a lifespan
348 (Pradeu and Eric, 2014), and thus that host immune system would not exert any pressure on
349 the resident microbiota. In this case, any changes in host immune response to infection would
350 potentially not affect the resident microbiota diversity and composition.
351 Interestingly, numerous studies demonstrate a direct control of microbial communities by the
352 host immune system. As an example, species-specific antimicrobial peptides can shape species-
353 specific bacterial associations in *Hydra* (Franzenburg et al., 2013). Other immune pathways
354 have been also demonstrated to regulate or control the microbiota communities, like the
355 intestinal homeo-box gene Caudal in *Drosophila* (Ryu et al., 2008), or neuropeptides with
356 antibacterial activity which are secreted to shape the microbiome on the body surface of *Hydra*
357 (Augustin et al., 2017), even host lectins were demonstrated to stabilize microbiota
358 communities (Dinh et al., 2018).
359 Thus, if biotic stress (i.e. an infection) modifies the expression of antimicrobial peptides or
360 other immune related pathways, an effect on the microbial communities can be expected. Our
361 results indicate that bacterial communities could indeed be shaped by the immune system of *B.*
362 *glabrata*. Based on the hypothesis proposed by Hooper and collaborators (Hooper and
363 Macpherson, 2010; Hooper et al., 2012; Dinh et al., 2018), it seems that the immune system of
364 *B. glabrata* snails maintains or controls the microbial communities permanently. Therefore,
365 following an infection, the immune system is diverted from its function of managing the
366 microbiota and consequently the bacterial communities evade its regulation, resulting in

bioRxiv preprint doi: https://doi.org/10.1101/386623; this version posted June 4, 2019. The copyright holder for this preprint (which was not certified by peer review) is the author/funder. All rights reserved. No reuse allowed without permission.

367 changes of their composition and diversity. When the immune response returns to a basal level,
368 the microbiota is again under-control and the microbiota shows its resilience by returning to its
369 "healthy" state (Hooper and Macpherson, 2010; Hooper et al., 2012), as observed in the
370 present study (Fig. 4). In other words, the immune system is likely no longer able to maintain
371 the microbiota homeostasis after infection (resulting in dysbiosis), which, may in turn affect
372 host homeostasis or fitness (Contijoch et al., 2019; Warne et al., 2019) (Contijoch, Britton et al.
373 2019, Warne, Kirschman et al. 2019).
374 Changes in microbiota composition may result from shifts in the abundance of specific bacterial
375 groups participating in anti-pathogen response, or just be a collateral effect of the immune
376 response activation against metazoan parasite infection. This question will deserve further
377 investigation, by testing *S. mansoni* prevalence and intensity in experimental infections of
378 *Biomphalaria glabrata* snails following antibiotic treatment or microbiota transplantation.
379
380 In order to fully understand Schistosomiasis transmission and to develop new ways to
381 control the expansion of this widespread human parasitic disease in the field, it will be crucial
382 to determine if the snail-associated bacterial communities affect the parasite transmission. For
383 example, expanding knowledge on *Biomphalaria* snail microbiota is an essential step for
384 developing paratransgenetic solutions to the spread of Schistosomiasis, involving the use of
385 transgenic bacteria expressing foreign gene products (i.e., schistosomicidal compounds) that
386 can reduce host competence and block pathogen development or transmission when
387 introduced into the microbiota of vector snail field populations (Aksoy et al., 2008; Coutinho-
388 Abreu et al., 2010; Gilbert et al., 2016).
389

bioRxiv preprint doi: https://doi.org/10.1101/386623; this version posted June 4, 2019. The copyright holder for this preprint (which was not certified by peer review) is the author/funder. All rights reserved. No reuse allowed without permission.

Experimental procedures

Ethical statements

Our laboratory holds permit # A66040 for experiments on animals, which was obtained from the French Ministry of Agriculture and Fisheries and the French Ministry of National Education, Research, and Technology. The housing, breeding and care of the utilized animals followed the ethical requirements of our country. The experimenter possesses an official certificate for animal experimentation from both of the above-listed French ministries (Decree # 87–848, October 19, 1987). The various protocols used in this study have been approved by the French veterinary agency of the DRAAF Languedoc-Roussillon (Direction Régionale de l'Alimentation, de l'Agriculture et de la Forêt), Montpellier, France (authorization # 007083).

Biological material

In this study, we used a single strain of the host snail, the albino Brazilian strain of *Biomphalaria glabrata* (BgBRE) and two strains of the trematode parasite *Schistosoma mansoni*: a Brazilian strain (SmBRE, for sympatric infection) and a Venezuelan strain (SmVEN, for allopatric infection). BgBRE and SmBRE strains originate from the locality of Recife, Brazil; the SmVEN parasite strain was recovered from the locality of Guacara, Venezuela. All host and parasite strains were maintained in the laboratory on their respective sympatric snail hosts (SmBRE on BgBRE and SmVEN on BgVEN). The snails were reared at constant temperature of 26°C and fed only with washed salad every 3 days.

Experimental Infections (Fig. 1)

In order to decipher the inter-individual structure of snail microbiota as well as investigate the

bioRxiv preprint doi: https://doi.org/10.1101/386623; this version posted June 4, 2019. The copyright holder for this preprint (which was not certified by peer review) is the author/funder. All rights reserved. No reuse allowed without permission.

413 influence of different snail immune stimulations on its microbiota structure and dynamics, we
414 applied a two-step experimental infection protocol (Fig. 1).
415 Briefly, BgBRE snails were primo-infected with one of the two parasite strains (SmBRE
416 sympatric or SmVEN allopatric). The snails were then sampled 1 and 4 days following primo-
417 infection by both parasite strains and 25 days after primo-infection for SmBRE infection
418 condition. Then, the BgBRE snails primo-infected with SmBRE were challenged (25 days after
419 the primo-infection) with SmBRE or SmVEN parasite strains for homologous or heterologous
420 challenges respectively. The challenged snails were then sampled 1 and 4 days following
421 challenge (Fig. 1). For all experimental infections, the snails were individually exposed for 12h
422 to 10 miracidia in 5mL of pond water, thereafter snails were returned to the water tanks and
423 separated according to the parasite strain and infection conditions.
424
425 Infections and sampling for microbiota analysis
426 We performed a primo-infection of 63 BgBRE snails with either SmBRE (sympatric, 49 snails) or
427 SmVEN (allopatric, 14 snails) strains. Then, 25 days after the primo-infection, we challenged a
428 subset (28 snails) of SmBRE-primo-infected snails with either SmBRE (14 snails) (homologous
429 challenge) or SmVEN (14 snails) (heterologous challenge).
430 To examine the effect of primo-infection on the snail microbiota, we sampled 7 whole snails for
431 each infection combination on day one (named BB1 and BV1; the first letter refers to the
432 *Biomphalaria* strain BgBRE and the second letter refers to the origin of *S. mansoni* strains used
433 for primo-infection, SmBRE or SmVEN), on day four (BB4 and BV4), and on day twenty-five
434 (BB25, no SmVEN-infected snails were sampled on day 25) after the primo-infection. This BB25
435 sample is used as control for microbiota changes observed following challenge infections. Thus

bioRxiv preprint doi: https://doi.org/10.1101/386623; this version posted June 4, 2019. The copyright holder for this preprint (which was not certified by peer review) is the author/funder. All rights reserved. No reuse allowed without permission.

436 then, we sampled 7 whole-snails on day one after the challenge (BBB1 and BBV1; the third
437 letter refers to the origin of the *S. mansoni* strain used for the challenge, SmBRE or SmVEN) and
438 on day four (BBB4 and BBV4) after the challenge. In addition, we used 6 naive snails collected at
439 the beginning of the experiment (B0) and 6 naive snails collected at the time of challenge (i.e.
440 day 25, named B25) as controls to assess the variability and stability of the BgBRE snail's
441 bacterial communities in our breeding and rearing laboratory conditions. Snails were not fed 24
442 hours before the DNA extraction for metabarcoding analysis.
443
444 Infection and sampling for host antimicrobial immune response
445 We performed a primo-infection of 180 BgBRE snails with either SmBRE (sympatric, 140 snails)
446 or SmVEN (allopatric, 40 snails). Then, 25 days after infection, we challenged a subset (80
447 snails) of SmBRE-infected snails with either SmBRE (40 snails) (homologous challenge) or
448 SmVEN (40 snails) (heterologous challenge) (Portet et al., 2019).
449 To study the primo-infection transcriptomic immune response of the snail, we took 20 snails
450 pooled for each infection type on day one (BB1 and BV1), four (BB4 and BV4), and twenty-five
451 (BB25). After the challenge with SmBRE or SmVEN, we sampled 20 snails in each condition at
452 days 1 and 4. Then samples of day 1 and day 4 were mixed together into a single sample
453 referring to BBB or BBV. In addition, we used 2 pools of 30 naive snails (B0.1 and B0.2) to
454 establish the basal snail transcriptomic activity (Portet et al., 2019).
455
456 *Extraction and sequencing*
457 DNA extraction and 16S rDNA sequencing

bioRxiv preprint doi: https://doi.org/10.1101/386623; this version posted June 4, 2019. The copyright holder for this preprint (which was not certified by peer review) is the author/funder. All rights reserved. No reuse allowed without permission.

458 Immediately after sampling, snail shells were cleaned with alcohol and removed, whole snails
459 were then frozen in liquid nitrogen and grounded. The total DNA was extracted with DNeasy
460 Blood and Tissue Kit (Qiagen) according to the manufacturer's protocol. The DNA quantification
461 was performed by Qubit 2.0 Fluorometer, using dsRNA BR Assay kit. Individual 16S rDNA
462 amplicon libraries were generated using the 341F (CCTACGGGNGGCWGCAG) and 805R
463 (GACTACHVGGGTATCTAATCC) primers targeting the variable V3-V4 loops (Klindworth et al.,
464 2013). Paired-end sequencing with 250 bp read length was performed on the Illumina MiSeq
465 sequencing system (Genome Québec, Montréal, Québec, Canada) using the v2 chemistry
466 according to the manufacturer's protocol.
467
468 RNA extraction and transcriptomic sequencing
469 Immediately after sampling, snail shells were cleaned with alcohol and removed, then snails
470 were pooled according to infection type. Total RNA was extracted using TRIZOL (Sigma Life
471 Science, USA) according to the manufacturer's instructions. For BBB and BBV equimolar
472 amounts of RNA extracted from molluscs challenged at both 1 and 4 days were mixed together
473 into a single sample. mRNAs were sequenced in paired-end 72-bp read lengths, using the
474 mRNA-Seq kit for transcriptome sequencing on Illumina Genome Analyzer II (MGX-Montpellier
475 GenomiX, Montpellier, France).
476
477 *Microbiota analysis*
478 Data analysis of 16S sequences
479 The FROGS pipeline (Find Rapidly OTU with Galaxy Solution) implemented on a galaxy instance
480 (http://sigenae-workbench.toulouse.inra.fr/galaxy/) was used for data processing (Escudié et

bioRxiv preprint doi: https://doi.org/10.1101/386623; this version posted June 4, 2019. The copyright holder for this preprint (which was not certified by peer review) is the author/funder. All rights reserved. No reuse allowed without permission.

al., 2017). Briefly, paired reads were merged using FLASH (Magoc and Salzberg, 2011). After denoising and primer/adapters removal (Didion et al., 2017), de novo clustering was done using SWARM, which uses a local clustering threshold, with aggregation distance d=3 after denoising. Chimeras were removed using VSEARCH (Rognes et al., 2016). We filtered out the singletons and performed taxonomic assignment using Blast+ against the Silva database (release 128).

All statistical analyses were done using R v3.3.1 (R: a language and environment for statistical computing, 2008; R Development Core Team, R Foundation for Statistical Computing, Vienna, Austria [http://www.R-project.org]). We used the phyloseq R package for community composition analysis (McMurdie and Holmes, 2013) to infer alpha diversity metrics as well as beta diversity (between sample distance). Beta diversity was examined by Principal Coordinate Analysis (PCoA) using the Bray-Curtis distance matrices. We performed a Mann Whitney U test ($p<0.05$) to compare alpha diversity and one-way PERMANOVA with a Benjamini & Hochberg post-hoc to analyze beta diversity between the experimental groups. For all analyses, the threshold significance level was set at 0.05.

Analysis of core-microbiota

We defined the core-microbiota as the set of bacterial families that were present in 100% of the naive individuals excluding unknown or multi-affiliations at lower taxonomic ranks (Table S1). We then used the abundances of OTUs belonging to these families to examine the composition of the core-microbiota.

To check if the core-microbiota is affected by infection, we compared the abundance of core families between infected snails and naive conditions with a one-way PERMANOVA with a Benjamini & Hochberg post-hoc correction. Moreover, a frequency test was performed to determine which specific families were affected during infection. The number of significantly

bioRxiv preprint doi: https://doi.org/10.1101/386623; this version posted June 4, 2019. The copyright holder for this preprint (which was not certified by peer review) is the author/funder. All rights reserved. No reuse allowed without permission.

504 differentially represented families at each sampling day (1, 4 and 25 days after primo infections
505 and 1, 4 days after challenges) was calculated to assess the temporal variability during the
506 course of infection.
507
508 *Transcriptome analysis of antimicrobial immune response*
509 Antimicrobial response
510 An antimicrobial transcriptome was built from transcripts known to be involved in *Biomphalaria*
511 immune response against bacteria (antimicrobial peptides: biomphamacin or antimicrobial
512 proteins: LBP/BPI and achacin; see Table S2 for details). The full-length sequences of these
513 transcripts were recovered from GenBank and the *Biomphalaria* genome (Adema et al., 2017)
514 and joined in a subset that represents the antimicrobial transcriptome of *B. glabrata*. This
515 antimicrobial transcriptome was then concatenated with a de-novo assembled transcriptome
516 of *Biomphalaria* available in our laboratory (see (Dheilly et al., 2015; Pinaud et al., 2016;
517 Galinier et al., 2017) for details) and uploaded on the Galaxy server. Before concatenation, a
518 blastn (70 % identity and 90% coverage) was conducted to identify redundant transcripts across
519 the transcriptomes. Redundant transcripts were then discarded using CDhitEst to avoid
520 mapping errors and bias in read counts when using Bowtie2 package.
521 Differential expression analysis
522 High-quality reads (Phred score >29) were aligned to the concatenated transcriptome using
523 Bowtie2 (v.2.0.2), which was run locally on a Galaxy server. The DESeq2 (v2.12) R package was
524 used to identify differential expression levels between uninfected (B0.1 and B0.2) and infected
525 conditions (p value < 0.05).
526

bioRxiv preprint doi: https://doi.org/10.1101/386623; this version posted June 4, 2019. The copyright holder for this preprint (which was not certified by peer review) is the author/funder. All rights reserved. No reuse allowed without permission.

Acknowledgments

BG was supported by ANR JCJC INVIMORY (number ANR 13-JSV7-0009) from the French National Research Agency (ANR). The authors want to thanks the DHOF program of the UMR5244/IHPE (http://ihpe.univ-perp.fr/en/ihpe-transversal-holobiont/) for partial financial support. This study is set within the framework of the "Laboratoires d'Excellences (LABEX)" TULIP (ANR-10-LABX-41).

Reference

Adema, C.M., Hillier, L.W., Jones, C.S., Loker, E.S., Knight, M., Minx, P. et al. (2017) Whole genome analysis of a schistosomiasis-transmitting freshwater snail. *Nature communications* **8**: 15451.

Aksoy, S., Weiss, B., and Attardo, G. (2008) Paratransgenesis applied for control of tsetse transmitted sleeping sickness. *Adv Exp Med Biol* **627**: 35-48.

Allan, E.R.O., Tennessen, J.A., Sharpton, T.J., and Blouin, M.S. (2018) Allelic Variation in a Single Genomic Region Alters the Microbiome of the Snail Biomphalaria glabrata. *J Hered* **109**: 604-609.

Astudillo-García, C., Bell James, J., Webster Nicole, S., Glasl, B., Jompa, J., Montoya Jose, M., and Taylor Michael, W. (2017) Evaluating the core microbiota in complex communities: A systematic investigation. *Environmental Microbiology* **19**: 1450-1462.

Augustin, R., Fraune, S., and Bosch, T.C.G. (2010) How Hydra senses and destroys microbes. *Seminars in Immunology* **22**: 54-58.

Augustin, R., Schröder, K., Murillo Rincón, A.P., Fraune, S., Anton-Erxleben, F., Herbst, E.-M. et al. (2017) A secreted antibacterial neuropeptide shapes the microbiome of Hydra. *Nature communications* **8**: 698.

bioRxiv preprint doi: https://doi.org/10.1101/386623; this version posted June 4, 2019. The copyright holder for this preprint (which was not certified by peer review) is the author/funder. All rights reserved. No reuse allowed without permission.

551 Bosch, T.C. (2013) Cnidarian-microbe interactions and the origin of innate immunity in
552 metazoans. *Annu Rev Microbiol* **67**: 499-518.
553 Bouchut, A., Roger, E., Gourbal, B., Grunau, C., Coustau, C., and Mitta, G. (2008) The
554 compatibility polymorphism in invertebrate host/trematode interactions: research of molecular
555 determinants. *Parasite* **15**: 304-309.
556 Budachetri, K., and Karim, S. (2015) An insight into the functional role of thioredoxin reductase,
557 a selenoprotein, in maintaining normal native microbiota in the Gulf Coast tick (Amblyomma
558 maculatum). *Insect Mol Biol* **24**: 570-581.
559 Chen, F., Krasity, B.C., Peyer, S.M., Koehler, S., Ruby, E.G., Zhang, X., and McFall-Ngai, M.J.
560 (2017) Bactericidal Permeability-Increasing Proteins Shape Host-Microbe Interactions. *mBio* **8**:
561 e00040-00017.
562 Cirimotich, C.M., Dong, Y., Clayton, A.M., Sandiford, S.L., Souza-Neto, J.A., Mulenga, M., and
563 Dimopoulos, G. (2011) Natural microbe - mediated refractoriness to Plasmodium infection in
564 Anopheles gambiae. *Science* **332**: 855-858.
565 Contijoch, E.J., Britton, G.J., Yang, C., Mogno, I., Li, Z., Ng, R. et al. (2019) Gut microbiota density
566 influences host physiology and is shaped by host and microbial factors. *Elife* **8**: pii: e40553.
567 Coustau, C., Gourbal, B., Duval, D., Yoshino, T.P., Adema, C.M., and Mitta, G. (2015) Advances in
568 gastropod immunity from the study of the interaction between the snail Biomphalaria glabrata
569 and its parasites: A review of research progress over the last decade. *Fish & Shellfish*
570 *Immunology* **46**: 5-16.
571 Coutinho-Abreu, I.V., Zhu, K.Y., and Ramalho-Ortigao, M. (2010) Transgenesis and
572 paratransgenesis to control insect-borne diseases: current status and future challenges.
573 *Parasitol Int* **59**: 1-8.

bioRxiv preprint doi: https://doi.org/10.1101/386623; this version posted June 4, 2019. The copyright holder for this preprint (which was not certified by peer review) is the author/funder. All rights reserved. No reuse allowed without permission.

574 Dheilly, N.M., Duval, D., Mouahid, G., Emans, R., Allienne, J.-F., Galinier, R. et al. (2015) A family
575 of variable immunoglobulin and lectin domain containing molecules in the snail Biomphalaria
576 glabrata. *Developmental & Comparative Immunology* **48**: 234-243.
577 Didion, J.P., Martin, M., and Collins, F.S. (2017) Atropos: specific, sensitive, and speedy
578 trimming of sequencing reads. *PeerJ* **5**: e3720.
579 Dinh, C., Farinholt, T., Hirose, S., Zhuchenko, O., and Kuspa, A. (2018) Lectins modulate the
580 microbiota of social amoebae. *Science* **361**: 402-406.
581 Doenhoff, M.J., Hagan, P., Cioli, D., Southgate, V., Pica-Mattoccia, L., Botros, S. et al. (2009)
582 Praziquantel: its use in control of schistosomiasis in sub-Saharan Africa and current research
583 needs. *Parasitology* **136**: 1825-1835.
584 Ducklow, H.W., Boyle, P.J., Maugel, P.W., Strong, C., and Mitchell, R. (1979) Bacterial flora of
585 the schistosome vector snail Biomphalaria glabrata. *Applied and Environmental Microbiology*
586 **38**: 667-672.
587 Escudié, F., Auer, L., Bernard, M., Mariadassou, M., Cauquil, L., Vidal, K. et al. (2017) FROGS:
588 Find, Rapidly, OTUs with Galaxy Solution. *Bioinformatics*: btx791.
589 Fallon, P.G., and Doenhoff, M.J. (1994) Drug-Resistant Schistosomiasis: Resistance to
590 Praziquantel and Oxamniquine Induced in Schistosoma Mansoni in Mice is Drug Specific. *The*
591 *American Journal of Tropical Medicine and Hygiene* **51**: 83-88.
592 Franzenburg, S., Fraune, S., Künzel, S., Baines, J.F., Domazet-Lošo, T., and Bosch, T.C.G. (2012)
593 MyD88-deficient Hydra reveal an ancient function of TLR signaling in sensing bacterial
594 colonizers. *Proceedings of the National Academy of Sciences of the United States of America*
595 **109**: 19374-19379.

bioRxiv preprint doi: https://doi.org/10.1101/386623; this version posted June 4, 2019. The copyright holder for this preprint (which was not certified by peer review) is the author/funder. All rights reserved. No reuse allowed without permission.

596 Franzenburg, S., Walter, J., Künzel, S., Wang, J., Baines, J.F., Bosch, T.C.G., and Fraune, S. (2013)
597 Distinct antimicrobial peptide expression determines host species-specific bacterial
598 associations. *Proceedings of the National Academy of Sciences of the United States of America*
599 **110**: E3730-E3738.
600 Fraune, S., Augustin, R., Anton-Erxleben, F., Wittlieb, J., Gelhaus, C., Klimovich, V.B. et al. (2010)
601 In an early branching metazoan, bacterial colonization of the embryo is controlled by maternal
602 antimicrobial peptides. *Proceedings of the National Academy of Sciences of the United States of*
603 *America* **107**: 18067-18072.
604 Fujio-Vejar, S., Vasquez, Y., Morales, P., Magne, F., Vera-Wolf, P., Ugalde, J.A. et al. (2017) The
605 Gut Microbiota of Healthy Chilean Subjects Reveals a High Abundance of the Phylum
606 Verrucomicrobia. *Front Microbiol* **8**: 1221.
607 Futo, M., Armitage, S.A., and Kurtz, J. (2015) Microbiota Plays a Role in Oral Immune Priming in
608 Tribolium castaneum. *Front Microbiol* **6**: 1383.
609 Galinier, R., Roger, E., Moné, Y., Duval, D., Portet, A., Pinaud, S. et al. (2017) A multistrain
610 approach to studying the mechanisms underlying compatibility in the interaction between
611 Biomphalaria glabrata and Schistosoma mansoni. *PLOS Neglected Tropical Diseases* **11**:
612 e0005398.
613 Gendrin, M. (2017) A Swiss Army Knife to Cut Malaria Transmission. *Cell Host & Microbe* **22**:
614 577-579.
615 Gilbert, J.A., Medlock, J., Townsend, J.P., Aksoy, S., Ndeffo Mbah, M., and Galvani, A.P. (2016)
616 Determinants of Human African Trypanosomiasis Elimination via Paratransgenesis. *PLoS Negl*
617 *Trop Dis* **10**: e0004465.

bioRxiv preprint doi: https://doi.org/10.1101/386623; this version posted June 4, 2019. The copyright holder for this preprint (which was not certified by peer review) is the author/funder. All rights reserved. No reuse allowed without permission.

618 Hooper, L.V., and Macpherson, A.J. (2010) Immune adaptations that maintain homeostasis with
619 the intestinal microbiota. *Nat Rev Immunol* **10**: 159–169.
620 Hooper, L.V., Littman, D.R., and Macpherson, A.J. (2012) Interactions between the microbiota
621 and the immune system. *Science (New York, N.Y.)* **336**: 1268-1273.
622 Jenkins, T.P., Peachey, L.E., Ajami, N.J., MacDonald, A.S., Hsieh, M.H., Brindley, P.J. et al. (2018)
623 Schistosoma mansoni infection is associated with quantitative and qualitative modifications of
624 the mammalian intestinal microbiota. *Sci Rep* **8**: 12072.
625 Joshi, D., Pan, X., McFadden, M.J., Bevins, D., Liang, X., Lu, P. et al. (2017) The Maternally
626 Inheritable Wolbachia wAlbB Induces Refractoriness to Plasmodium berghei in Anopheles
627 stephensi. *Frontiers in Microbiology* **8**: 366.
628 Klindworth, A., Pruesse, E., Schweer, T., Peplies, J., Quast, C., Horn, M., and Glockner, F.O.
629 (2013) Evaluation of general 16S ribosomal RNA gene PCR primers for classical and next-
630 generation sequencing-based diversity studies. *Nucleic Acids Res* **41**: e1.
631 Lozupone, C.A., Stombaugh, J.I., Gordon, J.I., Jansson, J.K., and Knight, R. (2012) Diversity,
632 stability and resilience of the human gut microbiota. *Nature* **489**: 220-230.
633 Magoc, T., and Salzberg, S.L. (2011) FLASH: fast length adjustment of short reads to improve
634 genome assemblies. *Bioinformatics* **27**: 2957-2963.
635 McFall-Ngai, M., Hadfield, M.G., Bosch, T.C., Carey, H.V., Domazet-Loso, T., Douglas, A.E. et al.
636 (2013) Animals in a bacterial world, a new imperative for the life sciences. *Proc Natl Acad Sci U*
637 *S A* **110**: 3229-3236.
638 McMurdie, P.J., and Holmes, S. (2013) phyloseq: an R package for reproducible interactive
639 analysis and graphics of microbiome census data. *PLoS One* **8**: e61217.

bioRxiv preprint doi: https://doi.org/10.1101/386623; this version posted June 4, 2019. The copyright holder for this preprint (which was not certified by peer review) is the author/funder. All rights reserved. No reuse allowed without permission.

640 Mitta, G., Adema, C.M., Gourbal, B., Loker, E.S., and Theron, A. (2012) Compatibility
641 polymorphism in snail/schistosome interactions: From field to theory to molecular
642 mechanisms. *Dev Comp Immunol* **37**: 1-8.
643 Mitta, G., Gourbal, B., Grunau, C., Knight, M., Bridger, J.M., and Théron, A. (2017) Chapter
644 Three – The Compatibility Between Biomphalaria glabrata Snails and Schistosoma mansoni: An
645 Increasingly Complex Puzzle. *Advances in Parasitology* **97**: 111-145.
646 Mitta, G., Galinier, R., Tisseyre, P., Allienne, J.F., Girerd-Chambaz, Y., Guillou, F. et al. (2005)
647 Gene discovery and expression analysis of immune-relevant genes from Biomphalaria glabrata
648 hemocytes. *Developmental and comparative immunology* **29**: 393-407.
649 Mone, Y., Gourbal, B., Duval, D., Du Pasquier, L., Kieffer-Jaquinod, S., and Mitta, G. (2010) A
650 large repertoire of parasite epitopes matched by a large repertoire of host immune receptors in
651 an invertebrate host/parasite model. *PLoS Negl Trop Dis* **4**: pii: e813.
652 Moné, Y., Ribou, A.-C., Cosseau, C., Duval, D., Théron, A., Mitta, G., and Gourbal, B. (2011) An
653 example of molecular co-evolution: Reactive oxygen species (ROS) and ROS scavenger levels in
654 Schistosoma mansoni/Biomphalaria glabrata interactions. *International Journal for Parasitology*
655 **41**: 721-730.
656 Narasimhan, S., Schuijt, T.J., Abraham, N.M., Rajeevan, N., Coumou, J., Graham, M. et al. (2017)
657 Modulation of the tick gut milieu by a secreted tick protein favors Borrelia burgdorferi
658 colonization. *Nature communications* **8**: 184.
659 Nyholm, S.V., and McFall-Ngai, M.J. (2004) The winnowing: establishing the squid-vibrio
660 symbiosis. *Nat Rev Microbiol* **2**: 632-642.
661 Onchuru, T.O., and Kaltenpoth, M. (2019) Established cotton stainer gut bacterial mutualists
662 evade regulation by host antimicrobial peptides. *Appl Environ Microbiol* **pii: AEM.00738-19.** .

bioRxiv preprint doi: https://doi.org/10.1101/386623; this version posted June 4, 2019. The copyright holder for this preprint (which was not certified by peer review) is the author/funder. All rights reserved. No reuse allowed without permission.

663 Pinaud, S., Portela, J., Duval, D., Nowacki, F.C., Olive, M.-A., Allienne, J.-F. et al. (2016) A Shift
664 from Cellular to Humoral Responses Contributes to Innate Immune Memory in the Vector Snail
665 Biomphalaria glabrata. *PLOS Pathogens* **12**: e1005361.
666 Portet, A., Pinaud, S., Chaparro, C., Galinier, R., Dheilly, N.M., Portela, J. et al. (2019) Sympatric
667 versus allopatric evolutionary contexts shape differential immune response in Biomphalaria /
668 Schistosoma interaction. *PLoS Pathog* **15**: e1007647.
669 Pradeu, T., and Eric, V. (2014) The discontinuity theory of immunity. *Sci Immunol* **1**: 1-9.
670 Ramirez, J.L., Souza-Neto, J., Cosme, R.T., Rovira, J., Ortiz, A., Pascale, J.M., and Dimopoulos, G.
671 (2012) Reciprocal tripartite interactions between the Aedes aegypti midgut microbiota, innate
672 immune system and dengue virus influences vector competence. *PLOS Neglected Tropical*
673 *Diseases* **6**: 1-11.
674 Rodrigues, J., Brayner, F.A., Alves, L.C., Dixit, R., and Barillas-mury, C. (2010) Hemocyte
675 Differentiation Mediates Innate Immune Memory in Anopheles gambiae Mosquitoes. *Science*
676 **329**: 1353-1355.
677 Rognes, T., Flouri, T., Nichols, B., Quince, C., and Mahe, F. (2016) VSEARCH: a versatile open
678 source tool for metagenomics. *PeerJ* **4**: e2584.
679 Ryu, J.-H., Kim, S.-H., Lee, H.-Y., Bai, J.Y., Nam, Y.-D., Bae, J.-W. et al. (2008) Innate Immune
680 Homeostasis by the Homeobox Gene Caudal and Commensal-Gut
681 Mutualism in <em>Drosophila</em&gt. *Science* **319**: 777.
682 Sansone, C.L., Cohen, J., Yasunaga, A., Xu, J., Osborn, G., Subramanian, H. et al. (2015)
683 Microbiota-dependent priming of antiviral intestinal immunity in Drosophila. *Cell Host and*
684 *Microbe* **18**: 571-581.

bioRxiv preprint doi: https://doi.org/10.1101/386623; this version posted June 4, 2019. The copyright holder for this preprint (which was not certified by peer review) is the author/funder. All rights reserved. No reuse allowed without permission.

685 Silva, T.M., Melo, E.S., Lopes, A.C.S., Veras, D.L., Duarte, C.R., Alves, L.C., and Brayner, F.A.
686 (2013) Characterization of the bacterial microbiota of Biomphalaria glabrata (Say, 1818)
687 (Mollusca: Gastropoda) from Brazil. *Letters in Applied Microbiology* **57**: 19-25.
688 Tennessen, J.A., Théron, A., Marine, M., Yeh, J.-Y., Rognon, A., and Blouin, M.S. (2015)
689 Hyperdiverse Gene Cluster in Snail Host Conveys Resistance to Human Schistosome Parasites.
690 *PLoS Genetics* **11**: e1005067.
691 Wang, X.W., Xu, J.D., Zhao, X.F., Vasta, G.R., and Wang, J.X. (2014) A shrimp C-type lectin
692 inhibits proliferation of the hemolymph microbiota by maintaining the expression of
693 antimicrobial peptides. *J Biol Chem* **289**: 11779-11790.
694 Warne, R.W., Kirschman, L., and Zeglin, L. (2019) Manipulation of gut microbiota during critical
695 developmental windows affects host physiological performance and disease susceptibility
696 across ontogeny. *J Anim Ecol* **Epub ahead of print**.
697 WHO (2002) TDR Strategic Direction for Research: Schistosomiasis. *World Health Organization*
698 *Information*.
699 Xi, Z., Ramirez, J.L., and Dimopoulos, G. (2008) The Aedes aegypti toll pathway controls dengue
700 virus infection. *PLOS Pathogens* **4(7):e1000098**.
701 Yang, H.T., Yang, M.C., Sun, J.J., Shi, X.Z., Zhao, X.F., and Wang, J.X. (2016) Dual oxidases
702 participate in the regulation of intestinal microbiotic homeostasis in the kuruma shrimp
703 Marsupenaeus japonicus. *Dev Comp Immunol* **59**: 153-163.
704 Yang, H.T., Yang, M.C., Sun, J.J., Guo, F., Lan, J.F., Wang, X.W. et al. (2015) Catalase eliminates
705 reactive oxygen species and influences the intestinal microbiota of shrimp. *Fish Shellfish*
706 *Immunol* **47**: 63-73.

bioRxiv preprint doi: https://doi.org/10.1101/386623; this version posted June 4, 2019. The copyright holder for this preprint (which was not certified by peer review) is the author/funder. All rights reserved. No reuse allowed without permission.

707 Zhang, H., Sparks, J.B., Karyala, S.V., Settlage, R., and Luo, X.M. (2015) Host adaptive immunity
708 alters gut microbiota. *ISME J* **9**: 770-781.

709

710

711

712

713

bioRxiv preprint doi: https://doi.org/10.1101/386623; this version posted June 4, 2019. The copyright holder for this preprint (which was not certified by peer review) is the author/funder. All rights reserved. No reuse allowed without permission.

Legends to Figures

Fig. 1: Experimental protocol

Fig. 2: *Biomphalaria glabrata* microbiota characterization

Characterisation of the *Biomphalaria* bacterial microbiota of six naive snails recovered at the start of experimentation (B0.1; B0.2; B0.3; B0.4; B0.5 and B0.6) and 6 naive snails recovered 25 days after the start of experimentation (B25.1; B25.2; B25.3; B25.4; B25.5 and B25.6). A. Phylum level composition of the 20 most abundant OTUs phyla among the 12 naive snails. B. The Venn diagram represents the number of the 97 OTUs families which shared between the 6 naive snails at B0 (left Venn diagram), and between the 6 naive snails at B25 (right Venn diagram).

Fig. 3: Microbiota alpha Diversity

Boxplots of Chao1 and Shannon indices for all samples. For the Naive condition, B0 and B25 snails were pooled; BB: primo infection of BgBRE by SmBRE; BV: primo infection of BgBRE by SmVEN; BBB: primo infection of BgBRE by SmBRE and challenge by SmBRE; BBV: primo infection of BgBRE by SmBRE and challenge by SmVEN. The time point is mentioned with 1, 4 or 25 corresponding to the day after primo-infection or challenge. The differences between naive and infected conditions were tested with a Mann-Whitney U test and significant differences mentioned with "*".

Fig. 4: Beta diversity and bacterial communities following *Biomphalaria* infection

bioRxiv preprint doi: https://doi.org/10.1101/386623; this version posted June 4, 2019. The copyright holder for this preprint (which was not certified by peer review) is the author/funder. All rights reserved. No reuse allowed without permission.

737 Dynamics of the bacterial microbiota of *Biomphalaria glabrata* following *Schistosoma* primo-
738 infection and challenge. A. Functional diversity comparisons of *Biomphalaria* microbiota along
739 infection. Principal coordinate analysis of pairwise Bray-Curtis distances between all infection
740 type and time samples. Axes represent the two synthetic variables explaining the greatest
741 proportion of variation in the data set. The sample name indicated in the figure corresponds to
742 the centroid of all the biological replicates points of the respective experimental sample. B.
743 Phylum level composition of the 20 most abundant OTUs among all points of the kinetic. In this
744 representation, the replicate naive snails were pooled for more readability.
745
746 **Fig. 5: Differential gene expression of Biomphamacin antimicrobial peptides**
747 Log2FC (fold change) of antimicrobial immune transcripts between naive and infected snails
748 inferred from previous RNAseq analysis on the same experiment. A positive Log2 fold-change
749 indicates over-expression in infected snails compared to the naive snails. Antimicrobial peptide
750 families included 6 Biomphamacins (macin-like AMPs) consisting of 6 genes (shade of green).
751
752 **Fig. S1: Core Microbiota analysis**
753 Modifications of the bacterial core microbiota of *Biomphalaria glabrata* following *Schistosoma*
754 primo-infection and challenge. After a one-way Permanova with a Benjamini & Hochberg post-
755 hoc, a frequency test was realised to determine which specific families were affected during
756 infection. A. Proportion of OTU Families affected by infection are represented by colour circles.
757 The Venn diagram shows more precisely the specific impact of infections on the OTU families
758 partially influenced. B. Heatmap corresponding to all core microbiota with clustering on Familiy

bioRxiv preprint doi: https://doi.org/10.1101/386623; this version posted June 4, 2019. The copyright holder for this preprint (which was not certified by peer review) is the author/funder. All rights reserved. No reuse allowed without permission.

759 modification patterns between conditions. The scale of red correspond to ratio between naive
760 condition and each point of infection.
761
762 **Fig. S2: Differential gene expression of LBP/BPI and Achacin antimicrobial protein families**
763 Log2FC (fold change) of antimicrobial immune transcripts between naive and infected snails
764 inferred from previous RNAseq analysis on the same experiment. A positive Log2 fold-change
765 indicates over-expression in infected snails compared to the naive snails. Antimicrobial protein
766 families: LBP/BPIs (*Lipopolysaccharide-binding protein / Bactericidal Permeability-Increasing*
767 *protein*) consisting of 5 genes (in blue) and achacins consisting of 2 genes (in orange).
768
769
770
771

bioRxiv preprint doi: https://doi.org/10.1101/386623; this version posted June 4, 2019. The copyright holder for this preprint (which was not certified by peer review) is the author/funder. All rights reserved. No reuse allowed without permission.

Infection Phenotypes

Primo Infection

Challenge

BgBRE

Cellular Immune Response

Encapsulation

Miracidia to SpI

SpII clonal multiplication int SpI

SpII migration

Cercaria development into SpII

Cercaria shedding

Humoral Immune Response

Humoral killing

0 day

1 day

4 days

10 days

25 days

26 days

29 days

1 day

4 days

Naïve Snails

B0

B25

x10 SmBRE

BB1

BB4

BB25

BBB1

BBB4

x10 SmVEN

BV1

BV4

BBV1

BBV4

Sampling : 7 whole snails extracted individually / kinetic point

Microbiota Analysis

DNA Samples

Whole snail grinding in liquid nitrogen individually

Whole DNA extraction with commercial kit

16s library and sequencing

OTU Library

Metabarcoding 16S

Host Antimicrobial Immune Response

Naïve Snails

B0.1

B0.2

RNA Samples

BB1

BB4

BB25

BBB

BBV

Sampling : pool of 20 whole snails / point of kinetic

BV1

BV4

Whole snail grinding in liquid nitrogen pooled

Whole RNA TRIzol extraction

polyA purification

mRNA Library

RNA Sequencing

A

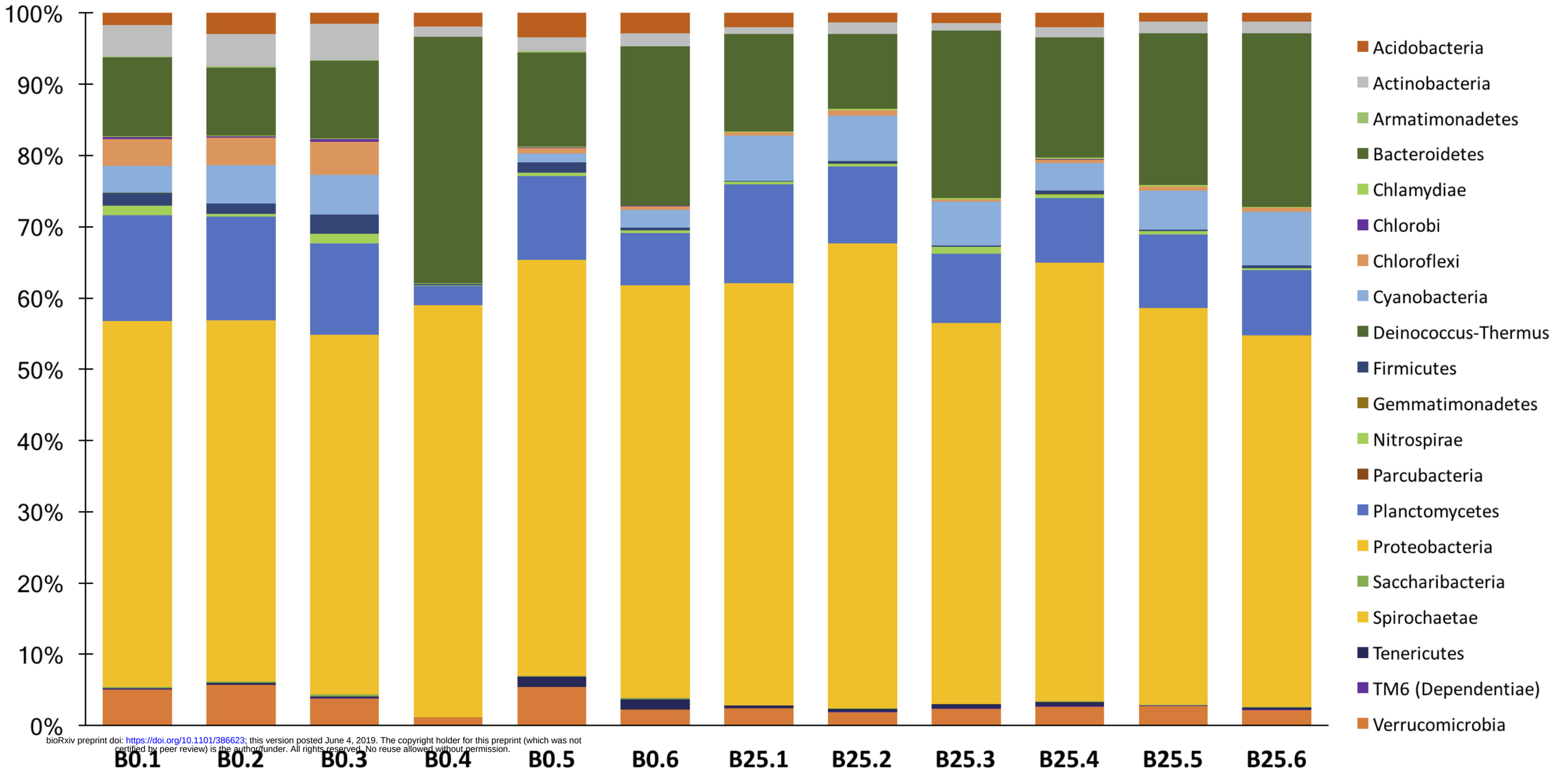

bioRxiv preprint doi: https://doi.org/10.1101/386623; this version posted June 4, 2019. The copyright holder for this preprint (which was not certified by peer review) is the author/funder. All rights reserved. No reuse allowed without permission.

B

bioRxiv preprint doi: https://doi.org/10.1101/386623; this version posted June 4, 2019. The copyright holder for this preprint (which was certified by peer review) is the author/funder. All rights reserved. No reuse allowed without permission.

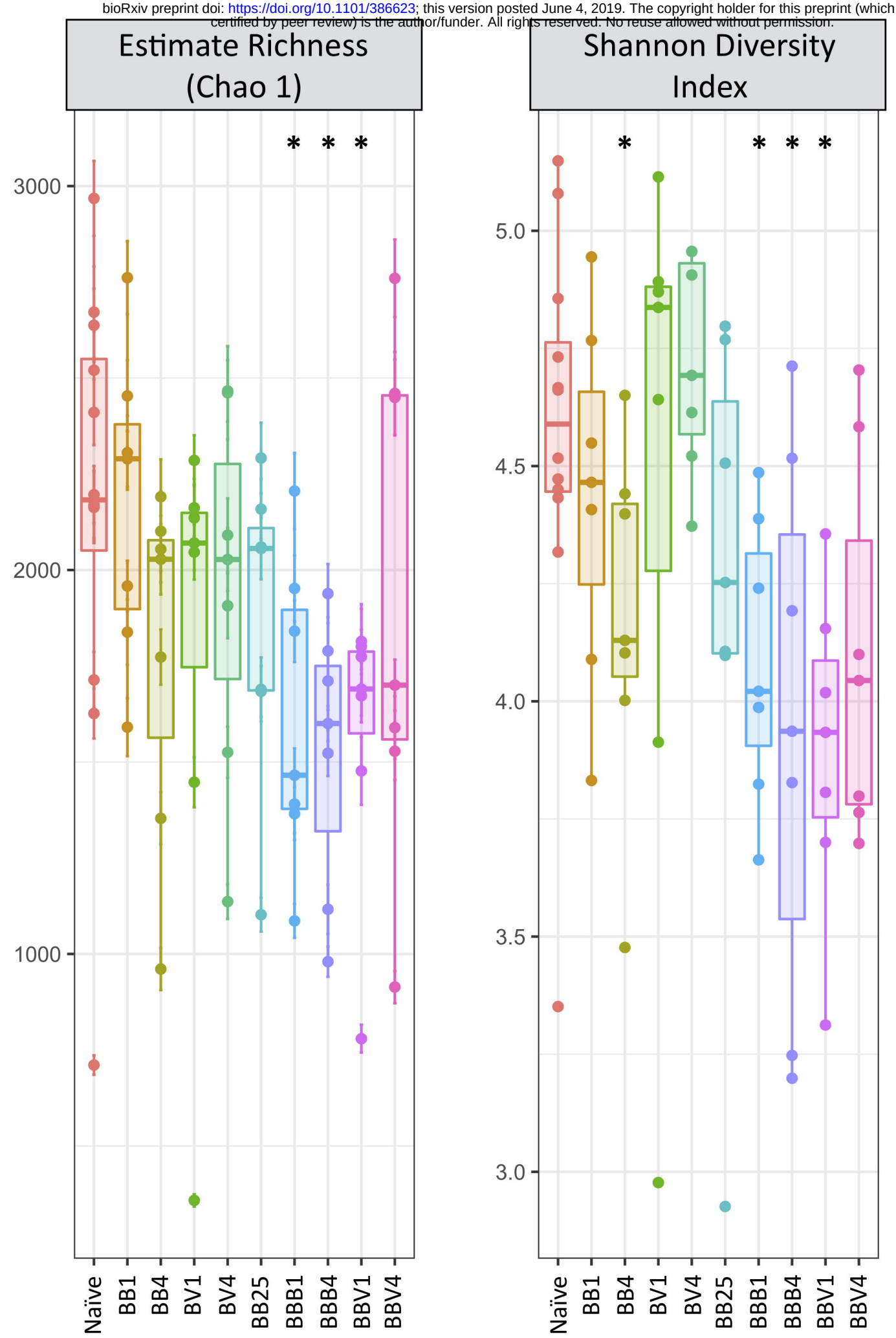

A

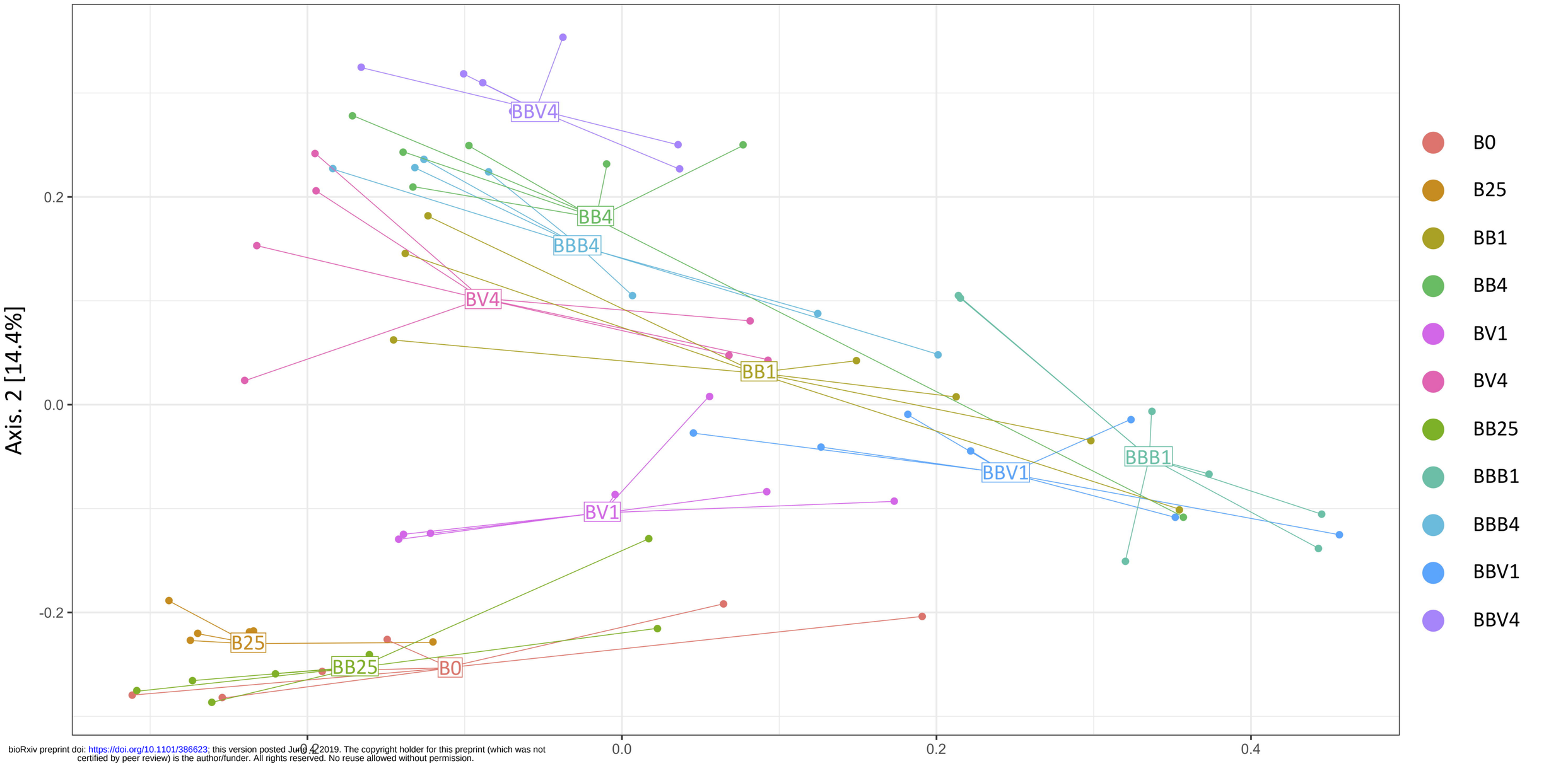

bioRxiv preprint doi: https://doi.org/10.1101/386623; this version posted June 4, 2019. The copyright holder for this preprint (which was not certified by peer review) is the author/funder. All rights reserved. No reuse allowed without permission.

B

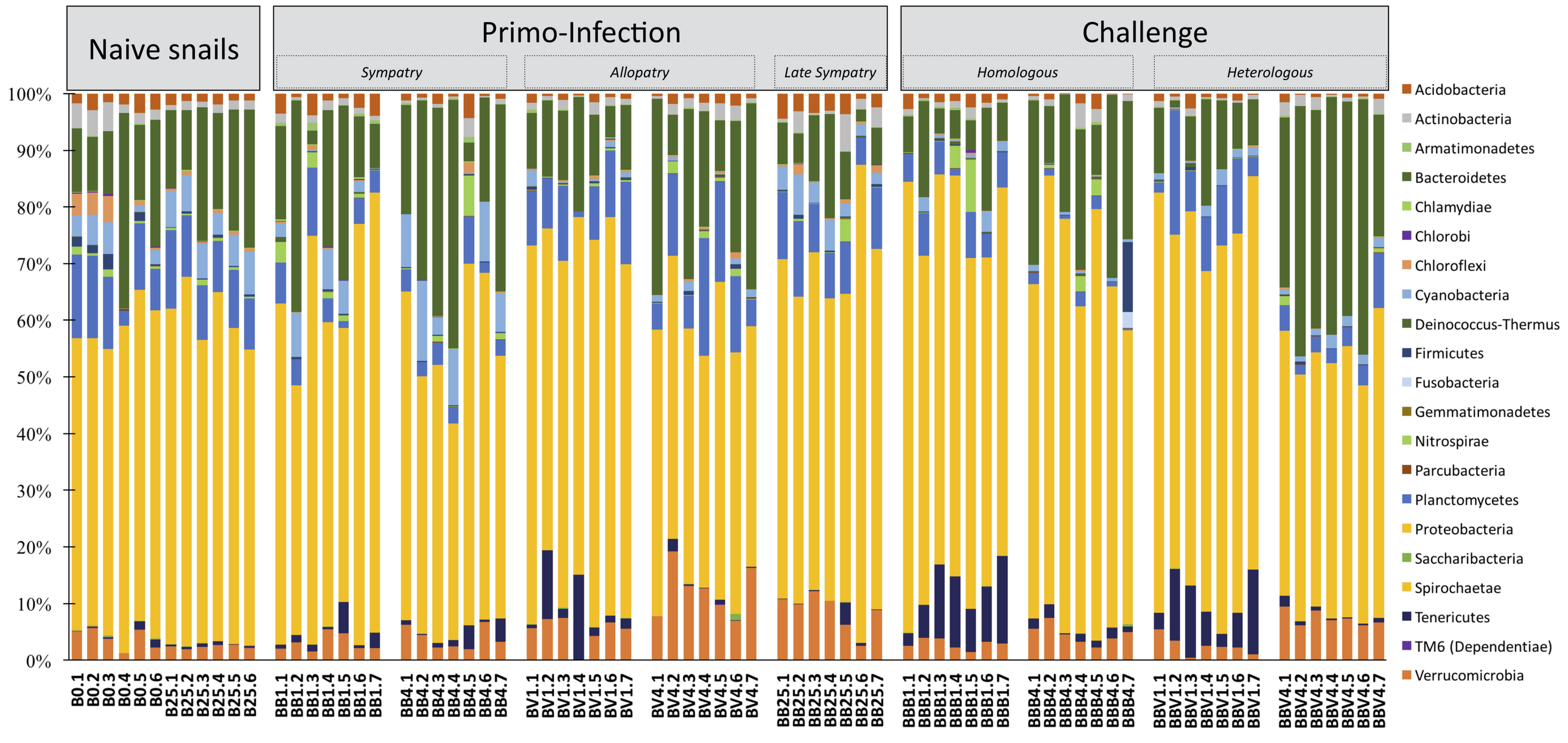

bioRxiv preprint https://doi.org/10.1101/386623; this version posted June 4, 2019. The copyright holder for this preprint (which was not certified by peer review) is the author/funder. All rights reserved. No reuse allowed without permission.